3.2 CEPC lattice design and Dynamic Aperture study

Yiwei Wang, Dou Wang, Yuan Zhang, Huiping Geng,

Sha Bai, Tianjian Bian, Feng Su, Jie Gao

Mail to: wangyw@ihep.ac.cn

Institute for High Energy Physics,

P.O. Box 918, Beijing 100049, China

3.2.1 Introduction

CEPC is a Circular Electron and Positron Collider proposed by China to mainly study the Higgs boson. In order to achieve factory luminosity, a strong focusing system and low emittance are required. A momentum acceptance as large as 2% is also required to get a reasonable beam lifetime. This is one of the key issues of the CEPC accelerator physics. In this paper, the optics design of the interaction and arc region and the optimization of dynamic aperture for the whole ring will be presented [1].

3.2.2 Single Ring Scheme

The parameters for single ring scheme of CEPC are shown in Tab.1.

3.2.2.1 *Interaction Region*

The CEPC interaction region (IR) was designed with modular sections [2–4] including the final transformer (FT), chromaticity correction for vertical plane (CCY), chromaticity correction for horizontal plane (CCX) and matching transformer (MT). To achieve a momentum acceptance as large as 2%, local correction of the large chromaticity from final doublet (FD) is necessary. Two pairs of sextupoles separated with -I transportation are used to make the 1st order chromaticity correction. The optics of the IR starting from the interaction point (IP) is shown in Fig.1.

To correct the tune shift due to finite length of main sextupoles, two pairs of weak sextupoles are installed next to the main ones [5]. The 1st order tune shift terms are shown in Fig.2.

To reduce the 2nd order chromaticity, the phases of sextupoles are carefully tuned. To reduce the 3rd order chromaticity, only 2 quadrupoles are used in the final transformer [6,7] and one additional sextupole are installed at 1^{st} image point [16]. Chromatic functions for the IR are shown in Fig.3. The change of the vertical tune is small than 0.03 when energy deviation dp/p=±2%. The horizontal plane can be optimized further with more additional sextupoles.

Table 1: Main parameters of CEPC single ring scheme [2]

Parameters	**Unit**	**Value**
Beam energy [E]	GeV	120
Circumference [C]	m	5,4374
Luminosity [L]	$cm^{-2}s^{-1}$	2.04×10^{34}
SR power/beam [P]	MW	51.7
Bending radius [ρ]	m	6094
Number of IP [N_{IP}]		2
Bunch number [n_B]		50
filling factor [κ]		0.7
Revolution period [T_0]	s	1.83×10^{-4}
momentum compaction factor [α_p]		3.36×10^{-5}
Energy acceptance Ring [h]		±0.02
lifetime due to radiative Bhabha scattering [τ_L]	min	50.61
Beam current [I]	mA	16.6
Bunch population [N_e]		3.79E+11
emittance-horizontal [$\varepsilon_{x,}\ \varepsilon_y$]	m· rad	6.12E-9, 1.84E-11
coupling factor [k]		0.003
Beam length SR [$\sigma_{s.SR}$]	mm	2.14
Beam length total [$\sigma_{s.tot}$]	mm	2.65
Betatron function at IP [$\beta_{x,}\ \beta_y$]	m	0.8, 0.0012
Transverse size [$\sigma_{x,}\ \sigma_y$]	μm	69.97, 0.15
Beam-beam parameter [$\xi_{x,}\ \xi_y$]		0.118, 0.083
Hourglass factor [Fh]		0.68
Lifetime due to Beamstrahlung-Telnov [τ_{BS}]	min	1005
Lifetime due to Beamstrahlung [simulation]	min	47
RF voltage [V_{rf}]	GV	6.87
RF frequency [f_{rf}]	GHz	0.65
Harmonic number [h]		118800

Synchrotron oscillation tune [ν_s]		0.18
Energy acceptance RF [h]	%	5.99
SR loss/turn [U_0]	GeV	3.11
Energy spread SR [$\sigma_{\delta.SR}$]	%	0.13
Energy spread BS [$\sigma_{\delta.BS}$]	%	0.09
Energy spread total [$\sigma_{\delta.tot}$]	%	0.16
Average number of photons emitted per electron during the collision [n_γ]		0.22
Transverse and Longitudinal damping time [n_x]	turns	78, 39

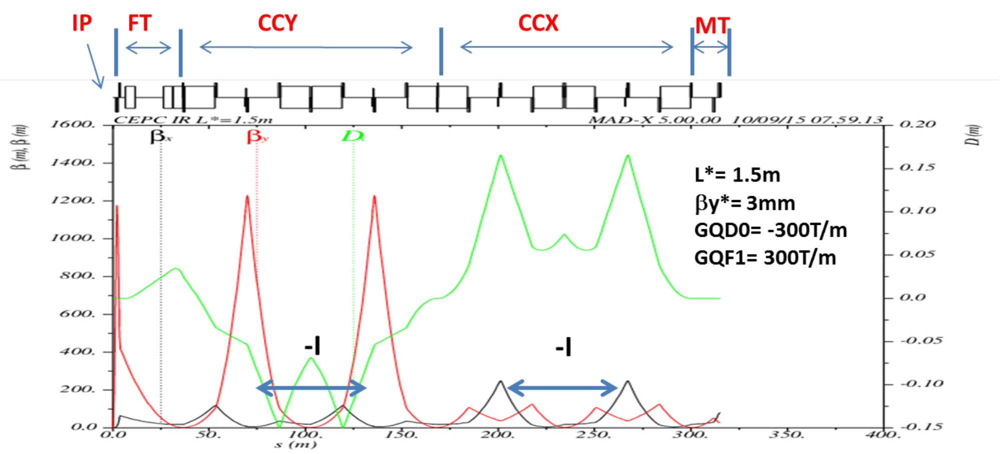

Figure 1: Optics of the interaction region (one side).

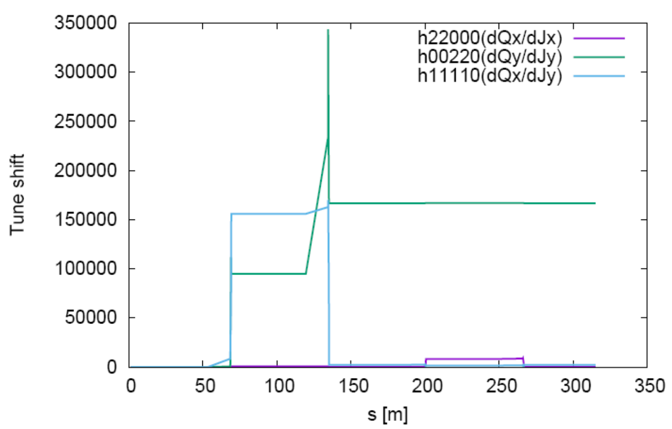

Figure 2: Tune shift correction in IR.

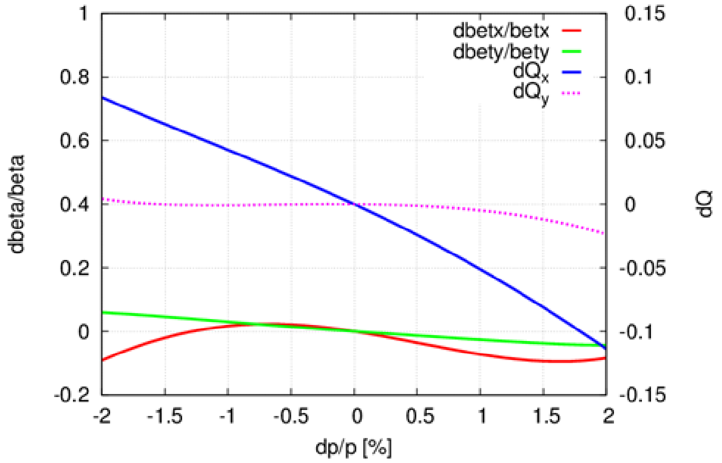

Figure 3: Chromatic functions at IP with the IR only (one side).

3.2.2.2 *Arc Region*

For the Arc region, the FODO cell structure is chosen to provide a large filling factor. The 60/60 degrees phase advances is selected due to its property of resonance cancellation [8, 9]. The 3rd and 4th order resonance driving terms (RDT) due to sextupoles in 24 cells is computed with Bengtsson's formular [11]. With only two families of sextupoles, all the 3rd and 4th order RDT except 2Qx −2Qy are cancelled out within one betatron unit, i.e. 6 cells. However, as Yunhai Cai pointed out that the tune shift accumulate along the arc cells and reach a very large number with the ring [8], see Fig.6. The negative tune shift make the tune of CEPC (0.08/0.22) go to the integer resonance line thus limit the on-momentum dynamic aperture (Fig. 4 and 5).

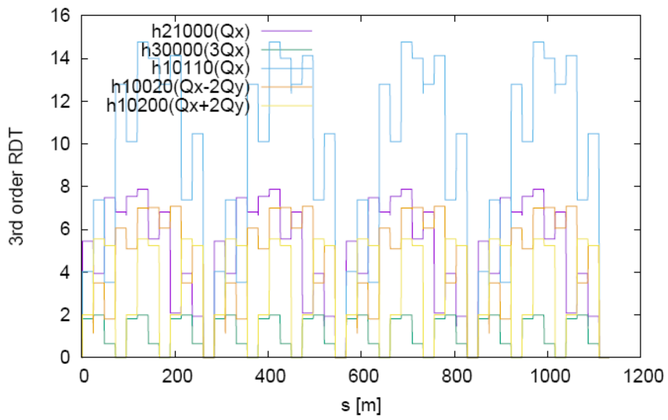

Figure 4: 3rd order resonance driving terms due to sextupoles in ARC (24cells).

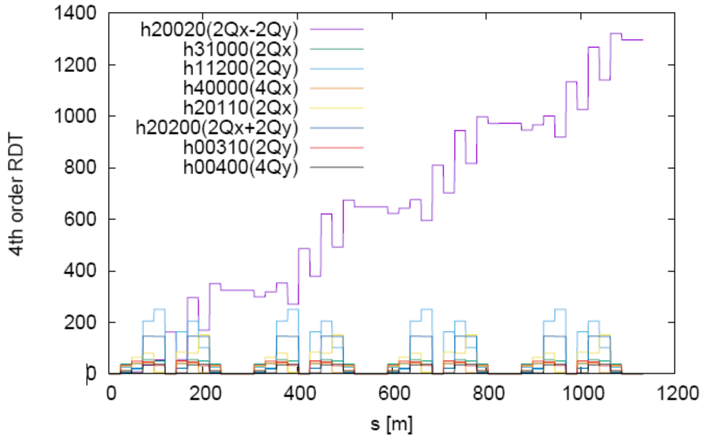

Figure 5: 4rd order resonance driving terms due to sextupoles in ARC (24cells).

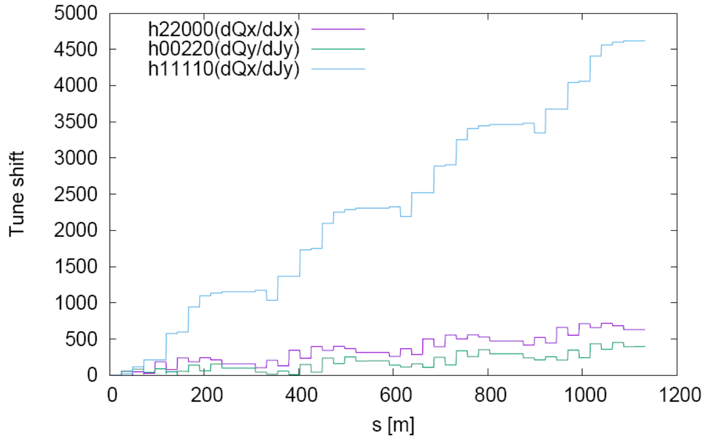

Figure 6: Tune shift due to sextupoles in ARC (24cells).

3.2.2.3 ***Dynamic Aperture***

Optimize DA with Additional Sextupoles in IR

In the previous CEPC IR lattice, many attempts have been tried to increase the dynamic aperture for off-momentum particles. With two pairs of main sextupoles separated by -I transportation, 2 pairs of weak sextupoles and one additional sextupole, the dynamic aperture of 3σx×20σy are achieved for dp/p=±2%, see Fig. 7. However, it's still not enough to keep a reasonable beam lifetime and luminosity which require 20σ for on momentum particles and 5σ for off momentum particles [10]. This section will show the further optimization of the DA for large off-momentum particles.

The previous DA result shown that DA drops quickly with momentum deviation even just ±0.5%. This is because of the breakdown of -I transportation. To correct this effect, a simple way is to correct the tiny chromaticity within the –I transportation. Thus we respectively put three sextupoles for the vertical and horizontal chromaticity correction section, i.e. the position (3,4,5) and (8,9,10). And three more sextupoles (2,6,7) help to correct the second order dispersion and so on. The positions of additional sextupoles are shown in Fig. 8. 1 denotes the sextupole we have added in previous IR lattice.

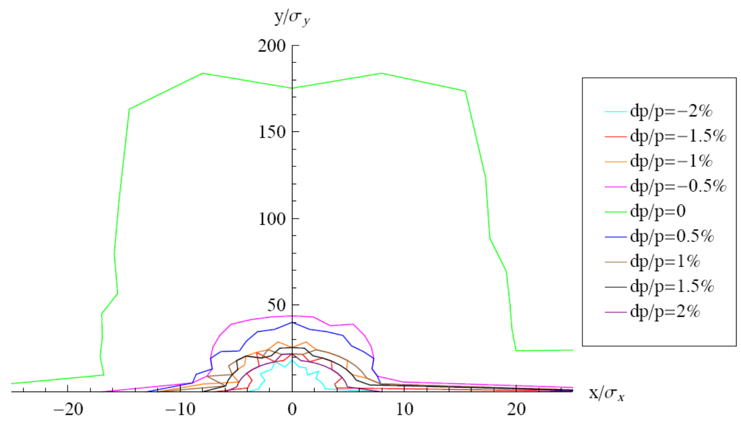

Figure 7: Dynamic aperture.

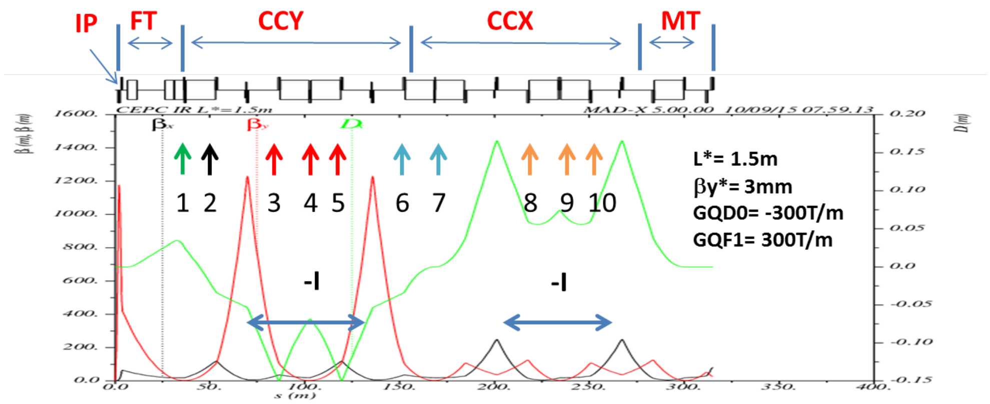

Figure 8: Optics of the interaction region with Brinkmann sextupoles.

It's difficult to correct a high order aberration while not increase other aberration. Similar to final focus of linear collider, we optimize the momentum acceptance directly in the following way [12]: In the plane of "DA vs. DP/P", the area of dynamic aperture with |dP/P| ⩽ 2% was got by tracking. A small coupling factor of 0.1% used to mainly optimize the horizontal DA. To avoid DA cut-in shape with small step of momentum deviation, as large as 19 points within |dP/P| ⩽ 2% were used. Four cases of initial phases, i.e. (0,0), (π/2,π/2), (0,π/2), (π/2,0) are considered. We maximize the area of four cases with Downhill Simplex algorithm [12]. The tracking was done with 100 turns which corresponding to around one damping time.

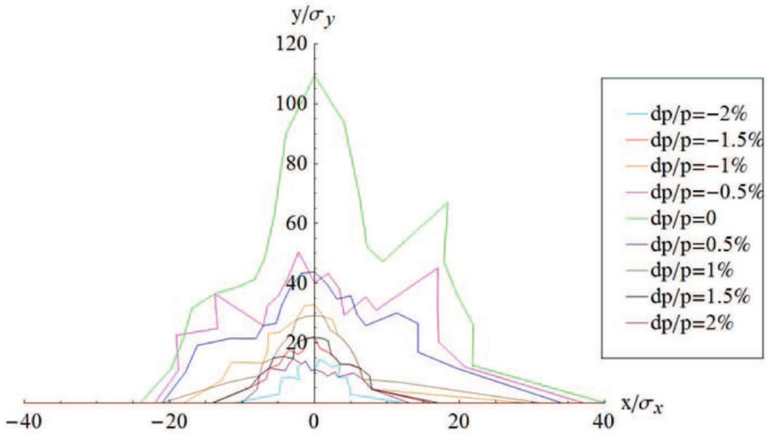

Figure 9: Dynamic aperture with Brinkmann sextupoles.

Fig. 9 shows the optimized dynamic aperture with Brinkmann sextupoles including synchrotron motion but without radiation damping and errors. The horizontal DA no longer drops quickly with momentum deviation. With dP/P = ±0.5%, the DA is still the same with on-momentum one, i.e. 20σx. The horizontal DA for dP/P = ±2% are significantly increased to around 6.5σx though the vertical one decreased to 10σy. This result has met the DA requirement we mentioned. Though thin sextuples are used in this study, there will be no significant finite length effect due to the weak sextupole strength.

Optimize DA with large families of sextupoles in ARC

We also optimized DA with large families of sextupoles in ARC by applying the differential evolution algorithm [13].

The x-z aperture of the original lattice is shown in Fig. 10, where the coupling is 0.3 %. There are only one family for SF/SD in the arc of the original lattice. Since the arc cell consists of 60/60 degree FODO lattice, we set the sextupole interleaved 180 degree one pair and there are totally 240 sextupole pairs used in the optimization. The objectives are listed in the following:

1. The tune Qx is in the range of [0.05, 0.31] and Qy in [0.10,0.31] for $\delta \in$ [-0.02, 0.02].

2. X-Z aperture objective is defined as an ellipse $\frac{x^2}{20^2}+\frac{z^2}{16^2}=1$, where x is the transverse amplitude in unit of RMS size with 0.3% coupling, and z is unit of RMS energy spread.

3. X-Y-Z aperture objective is defined as an elliptical ball $\frac{x^2}{20^2}+\frac{y^2}{50^2}+\frac{z^2}{16^2}=1$.

The optimized solution seems enlarge the dynamic aperture significantly, as shown in Fig. 11.

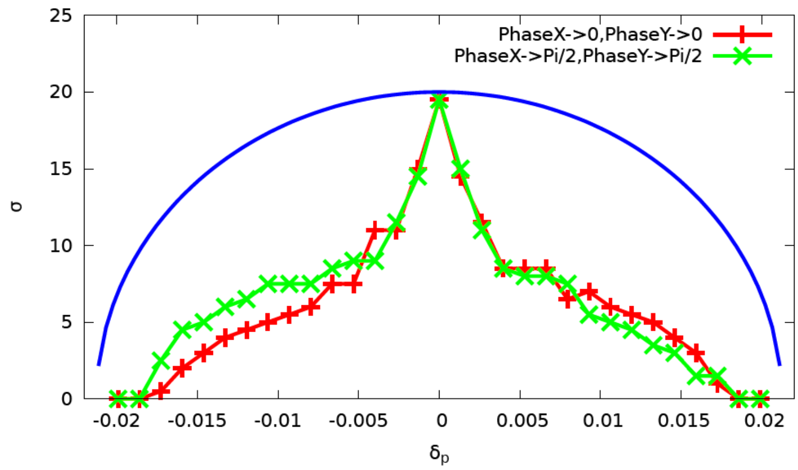

Figure 10: Dynamic aperture of CEPC before optimization.

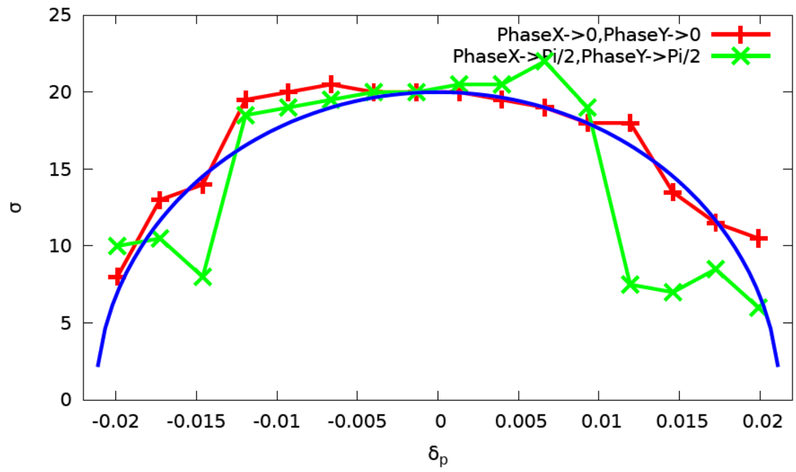

Figure 11: Dynamic aperture of CEPC after optimization.

Since there exist strong synchrotron radiation in the higgs factory, the radiation effect on DA should be also studied. The tracking shows that the damping really helps especially for large momentum offset particle, but the quantum fluctuation may reduce the DA for small momentum offset particle.

3.2.3 Partial Double Ring Scheme

In Pre-CDR, CEPC is a single ring machine [2]. All 50 bunches are equally spaced, and the collisions are head-on. This design requires a pretzel orbit in order to avoid parasitic collisions in the arcs. From the experience of LEP and CESR, the pretzel orbit is difficult to operate and control, and is also difficult for injection. After Pre-CDR, we developed a new idea called partial double ring scheme showed in Fig.12. Therefore, a pretzel orbit is not needed. With partial double ring scheme, we can consider crab waist on CEPC. The most important advantage of crab waist is that the beam-beam limit can be increased greatly, see Tab. 2.

The lattice design and dynamic aperture optimization for partial double ring scheme is undergoing.

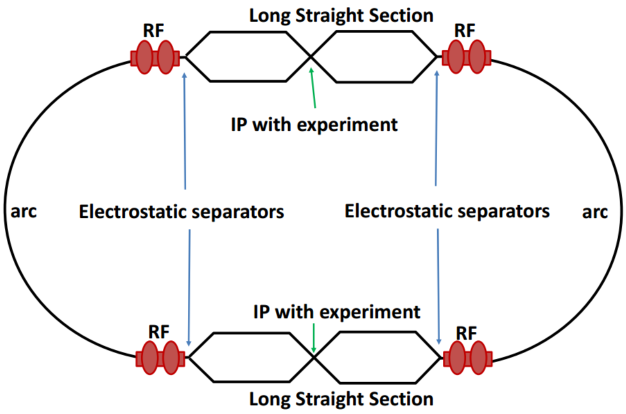

Figure 12: Dynamic aperture of CEPC after optimization [14].

Table 2: Main parameters of CEPC partial double ring scheme [15]

	Pre-CDR	H-high lumi.	H-low power	W	Z
Number of IPs	2	2	2	2	2
Energy (GeV)	120	120	120	80	45.5
Circumference (km)	54	54	54	54	54
SR loss/turn (GeV)	3.1	2.96	2.96	0.59	0.062
Half crossing angle (mrad)	0	15	15	15	15
Piwinski angle Φ	0	2.5	2.6	5	7.6
N_e/bunch (10^{11})	3.79	2.85	2.67	0.74	0.46
Bunch number	50	67	44	400	1100
Beam current (mA)	16.6	16.9	10.5	26.2	45.4
SR power /beam (MW)	51.7	50	31.2	15.6	2.8
Bending radius (km)	6.1	6.2	6.2	6.1	6.1
Momentum compaction (10^{-5})	3.4	2.5	2.2	2.4	3.5
β_{IP} x/y (m)	0.8/0.0012	0.25/0.00136	0.268 /0.00124	0.1/0.001	0.1/0.001
Emittance x/y (nm)	6.12/0.018	2.45/0.0074	2.06 /0.0062	1.02/0.003	0.62/0.0028
Transverse σ_{IP} (um)	69.97/0.15	24.8/0.1	23.5/0.088	10.1/0.056	7.9/0.053
ξ_x/IP	0.118	0.03	0.032	0.008	0.006
ξ_y/IP	0.083	0.11	0.11	0.074	0.073
V_{RF} (GV)	6.87	3.62	3.53	0.81	0.12
f_{RF} (MHz)	650	650	650	650	650
Nature σ_z (mm)	2.14	3.1	3.0	3.25	3.9
Total σ_z (mm)	2.65	4.1	4.0	3.35	4.0
HOM power/cavity (kw)	3.6	2.2	1.3	0.99	0.99
Energy spread (%)	0.13	0.13	0.13	0.09	0.05
Energy acceptance (%)	2	2	2		
Energy acceptance by RF (%)	6	2.2	2.1	1.7	1.1
n_γ	0.23	0.47	0.47	0.3	0.24
Life time due to beamstrahlung_cal (minute)	47	36	32		
F (hour glass)	0.68	0.82	0.81	0.92	0.95
L_{max}/IP ($10^{34}cm^{-2}s^{-1}$)	2.04	2.96	2.01	3.09	3.09

3.2.4 Acknowledgement

The authors would like to thank Y. Cai and K. Oide's beneficial discussion and help on the IR design and DA optimization. The authors also would like to thank K. Ohmi and D. Zhou's help on dynamic aperture simulation.

3.2.5 References

1. Y. Wang, Y. Zhang, S. Bai, et. al. , "Dynamic aperture study of the cepc main ring with interaction region", THPOR012, Proceedings of IPAC2016, Busan, Korea, May 2016.

2. The CEPC-SPPC Study Group, "CEPC-SPPC preliminary conceptual design report: volume II-accelerator", IHEP, Beijing, China, Rep. IHEP-AC-2015-01, Mar. 2015.

3. Y. Wang et al., in Proc. IPAC'15, pp. 2019-2021.

4. Y. Wang et al., "Optimization of the chromaticity correction section for CEPC FFS", IHEP, Beijing, China, Rep. IHEPAC-LC-Note2015-003, 2015.
5. A. Bogomyagkov et al., "Nonlinear properties of the FCC/TLEP final focus with respect to L*", Seminar at CERN, Mar. 2014.
6. K. Oide, "Final focus system for TLC", SLAC, USA, Rep. SLAC-PUB-4806, Nov. 1986.
7. Y. Cai, private communication, Apr. 2014.
8. Y. Cai, "Charged particle optics in circular Higgs factory", SLAC, USA, Rep. SLAC-PUB-16232, 2015.
9. K. L. Brown, "First and second order charged particle optics", SLAC, USA, Rep. SLAC-PUB-3381, Jul. 1984.
10. Y. Wang et. al., "Dynamic aperture optimization of CEPC with additional sextupoles in the interaction region", IHEP, Beijing, China, Rep. IHEP-AC-LC-Note2015-015, Dec. 2015.
11. J. Bengtsson, "The sextupole scheme for the Swiss light source (SLS): An analytic approach", PSI, Switzerland, Rep. SLS-Note-9-97, Mar. 1997.
12. K. Oide, private communication, Sep. 2015.
13. Y. Zhang, D. Zhou, "Application of differential evolution algorithm in future collider optimization", TUOBA03, Proceedings of IPAC2016, Busan, Korea, May 2016.
14. M. Koratzinos, "Mitigating performance limitations of single beam-pipe circular e + e − c colliders", TUPTY058, Proceedings of IPAC2015, Richmond, VA, USA, May 2015.
15. D. Wang, J. Gao, F. Su, M. Xiao, et al, "Parameter choice and partial double ring design", THPOR010, Proceedings of IPAC2016, Busan, Korea, May 2016.
16. R. Brinkmann, "Optimization of a final focus system for large momentum bandwidth", DESY, Germany, Rep. DESY-M-90-14, 1990.